Comparison of HONO budgets for two measurement heights at a field station within the Boreal Forest (SMEAR II – HUMPPA-COPEC-2010)

R. Oswald[1,2], M. Ermel[1,2], K. Hens[3], A. Novelli[3], H. G. Ouwersloot[3,4], P. Paasonen[5], T. Petäjä[5], M. Sipilä[5], P. Keronen[5], J. Bäck[6], R. Königstedt[3], Z. Hosaynali Beygi[3], H. Fischer[3], B. Bohn[7], D. Kubistin[3,8], H. Harder[3], M. Martinez[3], J. Williams[3],T. Hoffmann[2], I. Trebs[1*], and M. Sörgel[1]

[1] Biogeochemistry Department, Max Planck Institute for Chemistry, P.O. Box 3060, 55020 Mainz, Germany

[2] Institute for Inorganic and Analytical Chemistry, Johannes Gutenberg University Mainz, 55128 Mainz, Germany

[3] Airchemistry Department, Max Planck Institute for Chemistry, 55128 Mainz, Germany

[4] Meteorology and Air Quality, Wageningen University, Wageningen, The Netherlands

[5] Department of Physics, P.O. Box 64. 00014 University of Helsinki, Finland

[6] Department of Forest Sciences, P.O. Box 27, 00014 University of Helsinki, Finland

[7] Institut für Energie- und Klimaforschung IEK-8: Troposphäre, Forschungszentrum Jülich GmbH, 52428 Jülich, Germany

[8] University of Wollongong, School of Chemistry, Wollongong, Australia

[*] now at: Centre de Recherche Public - Gabriel Lippmann, Department Environment and Agro-biotechnologies, 41 rue du Brill, L-4422 Belvaux, Luxembourg

Correspondence to: m.soergel@mpic.de

1 **Abstract**

2 Atmospheric concentrations of nitrous acid (HONO), one of the major precursors of the

3 hydroxyl radical (OH) in the troposphere, significantly exceed the values predicted by the

4 assumption of a photostationary state (PSS) during daytime. Therefore, additional sources of

5 HONO were intensively investigated in the last decades. This study presents budget

6 calculations of HONO based on simultaneous measurements of all relevant species including

7 HONO and OH at two different measurement heights, i.e. 1 m above ground and about 2 to 3

8 m above canopy (24 m above ground), conducted in a Boreal forest environment. We

9 observed mean HONO concentrations during daytime of about 6.5×10^8 molecules cm^{-3} (26

10 ppt), more than twenty times higher than expected from the PSS, 0.2×10^8 molecules cm^{-3} (1

11 ppt). To close the budgets at both heights, a strong additional source term during daytime is

12 required. This unidentified source is maximal at noon (up to 1.1×10^6 molecules cm^{-3} s^{-1}, 160

13 ppt h^{-1}) and in general up to 2.3 times stronger above the canopy than close to the ground. The

14 insignificance of known gas phase reactions and also other processes like dry deposition or

15 advection, compared to the photolytic decomposition of HONO at this measurement site was

16 an ideal prerequisite to study possible correlations of this unknown term to proposed HONO

17 sources. But neither the proposed emissions from soils nor the proposed photolysis of

18 adsorbed HNO$_3$ contributed substantially to the unknown source. However, the unknown

19 source was found to be perfectly correlated to the unbalanced photolytic loss of HONO.

20

21 **1 Introduction**

22 Since the first unequivocal detection of HONO in the atmosphere by Perner and Platt (1979),

23 its formation and fate as well as its contribution to primary OH production has been

24 intensively studied (Lammel and Cape, 1996; Kleffmann, 2007). Recently, the importance of

25 HONO in atmospheric chemistry and its implications has been demonstrated using a global

26 chemistry transport model (Elshorbany et al., 2012). While the fate of HONO is mainly

27 determined by the photolytic decomposition producing OH, the major uncertainty in

28 modelling studies results from the lack of understanding the HONO formation pathways.

29 Budget calculations of the postulated sources and sinks (Kleffmann et al., 2005; Su et al.,

30 2008b; Sörgel et al., 2011a) have usually been used to quantify the magnitude of the missing

31 source term. Only a few source estimates derived from flux measurements have been

32 published up to now (Zhang et al., 2012; Zhou et al., 2011; Ren et al., 2011). The current

1 status of HONO formation and loss pathways, important for atmospheric chemistry is as

2 follows.

3 The major sink during daytime for HONO is the homolytic cleavage of the O-N single bond

4 by radiation ($\lambda < 400$ nm), determined by the photolysis frequency, J(HONO).

$$HONO \xrightarrow{h\nu} OH+NO \tag{R1}$$

5 Since OH is produced, this reaction is of primary importance to atmospheric photochemistry.

6 J(HONO) shows a similar wavelength dependency as the photolysis frequency of nitrogen

7 dioxide (NO_2), $J(NO_2)$ (Kraus and Hofzumahaus, 1998). Therefore J(HONO) can be linked to

8 $J(NO_2)$ by using the approach of Trebs et al. (2009):

$$J(HONO) = 0.17 \text{ x } J(NO_2) \tag{1}$$

9   The back reaction of (R1) in presence of a third body can reform HONO with a rate constant

10 (k_2 at 298 K and 1013 hPa) of (7.4 ± 1.3) x 10^{-12} cm^3 molecules^{-1} s^{-1} (reaction (R2)) (Sander et

11 al., 2011).

$$OH+NO \xrightarrow{M} HONO \tag{R2}$$

12 While the gas phase reaction of OH with NO forms HONO, OH may also react with HONO

13 and reform NO_x.

$$HONO+OH \rightarrow NO_2+H_2O \tag{R3}$$

14 Since concentrations of HONO and OH are generally much lower than those of NO, reaction

15 (R3) has less influence on HONO cycling than reaction (R2), although the reaction rate

16 constant (k_3 at 298 K and 1013 hPa) of about 6.0 x 10^{-12} cm^3 molecules^{-1} s^{-1} is similar

17 (Atkinson et al., 2004). Hence, the turnover is low and contributes typically less than 5 % to

18 the total HONO loss (Su et al., 2008b; Sörgel et al., 2011a).

19 A surface reaction of NO_2 and H_2O was suggested as another formation pathway for HONO.

20 Finlayson-Pitts et al. (2003) proposed a mechanism, whereby NO_2 is dimerized and then

21 dissolved in a humid surface film. The formed N_2O_4 rearranges into the mixed anhydride of

22 nitrous acid and nitric acid ($ONONO_2$), which rapidly dissolves into HONO and nitrate.

$$2NO_2(g)+H_2O(l) \rightarrow HONO(g)+H^+(aq)+NO_3^-(aq) \tag{R4}$$
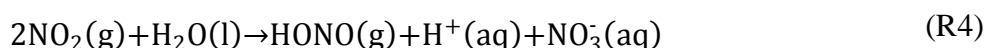
1 Yabushita et al. (2009) and De Jesus Medeiros and Pimentel (2011) further investigated the
2 mechanism with focus on the NO_2 uptake and the kinetics of the initial hydrolysis. The
3 reaction rate constant of reaction (R4) is difficult to determine in the field, but can be
4 estimated with the approach of Alicke et al. (2002).

$$k_4^{dark} = \frac{[HONO]_{max} - [HONO]_{sunset}}{(t_{max} - t_{sunset}) \times \overline{[NO_2]_{t_{sunset}}^{t_{max}}}} \qquad (2)$$

5 After sunset the concentration of HONO, $[HONO]_{sunset}$, increases and reaches a maximum,
6 $[HONO]_{max}$. The difference between $[HONO]_{max}$ and $[HONO]_{sunset}$ divided by the product of
7 the elapsed time (t_{max}-t_{sunset}) and the average NO_2 concentration during that time, $\overline{[NO_2]_{t_{sunset}}^{t_{max}}}$,
8 determines the rate of heterogeneous HONO formation during the night. The reaction rates
9 found for nighttime conversion range from 0.4 (Kleffmann et al., 2003) to 2.0 ppb(HONO) x
10 ppb(NO_2)$^{-1}$ x h^{-1} (Sörgel et al., 2011a). This approach is only valid, if the heterogeneous dark
11 reaction (R4) is the dominant source of HONO during night.

12 Beside the dark reaction of NO_2, ortho-nitrophenols, o-NPs, can photolytically decompose to
13 form HONO as a side product (Bejan et al., 2006).

$$\text{o-NPs} \xrightarrow{h\nu} [\text{products}]^* + HONO \qquad (R5)$$

14 The authors propose parts of the reaction mechanism, but since they could not measure the
15 main products, the exact and complete mechanism is not yet clarified. It is further stated that
16 this source might be of primary interest for the atmosphere under urban conditions, where
17 possibly 1 ppb of o-NPs occurs. Since the o-NPs absorb light in a similar wavelength range as
18 NO_2, it is possible to estimate the photolysis frequency (in s^{-1}) of o-NPs (J(o-NPs)) based on
19 measured relative photolysis frequencies of HONO formation from o-NPs and that of NO_2
20 (Bejan et al., 2006). This approach gives an upper limit for HONO formation from o-NPs.
21 J(NO_2) can be substituted by J(HONO) according to Eq. (1).

$$J(\text{o-NPs}) = 2.5 \times 10^{-3} \times J(NO_2) = 1.4 \times 10^{-2} \times J(HONO) \qquad (3)$$

22 In addition to the reaction of NO_2 with surface adsorbed water (R4), Stemmler et al. (2006)
23 and (2007) found that a surface film or aerosol of humic acid (HA) can act as photosensitizer
24 when irradiated and reduces NO_2 to HONO.

$$HA \xrightarrow{h\nu} A^{red} + X^{ox} \qquad (R6)$$

$$A^{red} + X^{ox} \rightarrow HA' \tag{R7}$$

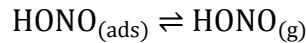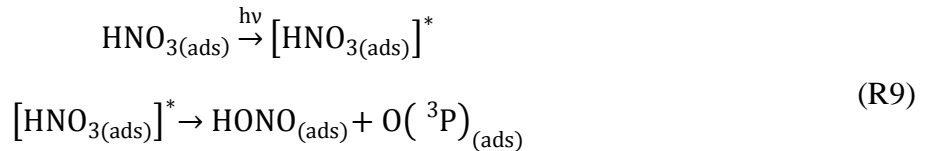$$A^{red} + NO_2 \rightarrow HA'' + HONO \tag{R8}$$

1   HA naturally occurs in the environment for example in soil. Hence, soil might act as a source

2   for HONO under irradiation in the UV and exposure to NO_2 (Stemmler et al., 2006). Other

3   reactants than A^{red} in reaction (R8) might also be reductive. E.g. fresh soot particles are

4   supposed to reduce NO_2 and form HONO. This source is only important for high NO_2

5   concentrations and environments with freshly emitted soot (Aubin and Abbatt, 2007; Monge

6   et al., 2010).

7   It was shown by several studies (Kubota and Asami, 1985; Twigg et al., 2011; Su et al., 2011;

8   Oswald et al., 2013) that soils can emit HONO. Decreasing soil water content and, hence,

9   drying out of soil leads to an increase in soil aeration with emission of trace gases, namely

10   N_2O, NO and HONO. Due to the complexity of soil emission fluxes, depending on biological,

11   physical and chemical processes as well as on soil properties, it is not straight forward to

12   calculate the source strength, although observed NO emissions might serve as a proxy for

13   HONO emission fluxes (Oswald et al., 2013). Furthermore, the exchange of HONO between

14   the soil and atmosphere may be influenced by accumulation of deposited HONO at the soil

15   surface and subsequent reemission during day (VandenBoer et al., 2013). This may lead to

16   enhanced emission of HONO compared to performed laboratory soil studies. Similar drying

17   leaf surfaces can release HONO from evaporating dew (He et al., 2006), which constitutes

18   another process related to drying surfaces.

19   Surface adsorbed nitric acid $HNO_{3(ads)}$ that is either deposited or directly formed during the

20   reaction cascade of (R4) was proposed to be photolytically sensitive and might decompose to

21   HONO in the UV (Zhou et al., 2011).

$$HNO_{3(ads)} \xrightarrow{h\nu} \left[HNO_{3(ads)}\right]^*$$

$$\left[HNO_{3(ads)}\right]^* \rightarrow HONO_{(ads)} + O\left(^3P\right)_{(ads)} \tag{R9}$$

$$HONO_{(ads)} \rightleftharpoons HONO_{(g)}$$

22   The production of HONO by photolysis of $HNO_{3(ads)}$ depends on the physicochemical state of

23   the surface. While for dry surfaces (relative humidity (RH) = 0%) NO_x is the major product,

24   relative humidity of about 20 % suffices to increase the HONO yield (Zhou et al., 2003).

According to Goodman et al. (2001), at 20 % RH at least a monolayer of water present should be on the surface. Zhou et al. (2003) further propose that $NO_{2(ads)}$ formed during the photolysis of $HNO_{3(ads)}$ may also react further via reaction (R4), which not only forms HONO, but also recovers parts of HNO_3. Later on, Zhou et al. (2011) suggested that the formed NO_2 is reduced to HONO via the mechanism of reaction (R6) and (R8) proposed by Stemmler et al. (2006). However, the rate of HONO formation depends on the amount of HNO_3 available on irradiated surfaces and the photolysis frequency of HNO_3, $J(HNO_3)$, which is enhanced by adsorption to surface compared to gas phase photolysis (Zhu et al., 2008; Zhu et al., 2010). Depending on the type of surface the enhancement factor varies; Zhou et al. (2003) found an enhancement of about 2 orders of magnitude by HNO_3 adsorption on borosilicate glass (see also Ramazan et al., 2004), while Baergen and Donaldson (2013) calculated an enhancement of about 4 orders of magnitude by HNO_3 adsorbed to grime.

Other loss terms than reactions (R1) and (R3) include the dry and wet deposition of HONO. The dry deposition of HONO depends on the ambient mixing ratio of HONO, on turbulent mixing within the planetary boundary layer and the ability of terrestrial surfaces to take up HONO. With a Henry coefficient of 49 M atm^{-1} (Park and Lee, 1988), wet deposition of HONO is quite efficient especially for neutral to alkaline solutions (effective Henry coefficient). Mixing ratios of HONO strongly decrease after a rain events (Sörgel et al., 2011b).

Assuming only the known gas phase reactions R1 to R3 contribute to the HONO formation, a photostationary state should be established (Kleffmann et al., 2005),

$$\frac{d[HONO]_{PSS}}{dt} = k_2[NO][OH] - J(HONO)[HONO]_{PSS} - k_3[OH][HONO]_{PSS} = 0 \tag{4}$$

$$\Rightarrow \quad [HONO]_{PSS} = \frac{k_2[NO][OH]}{J(HONO) + k_3[OH]} \tag{5}$$

This equilibrium can only explain a minor portion of gas phase HONO observed at remote and rural sites (Kleffmann, 2007; Su et al., 2008b; Sörgel et al., 2011a; Wong et al., 2012), but may play an important role for measurement results obtained in urban areas (Lee et al., 2013). The budget calculations of Sörgel et al. (2011a) and Li et al. (2012) showed that including heterogeneous reactions of NO_2 (R4) only slightly improves the discrepancy between $[HONO]_{PSS}$ and measured HONO mixing ratios.

1   In this study, we present the results of the field campaign HUMPPA-COPEC 2010 (<u>H</u>yytiälä

2   <u>U</u>nited <u>M</u>easurement of <u>P</u>hotochemistry and <u>P</u>articles in <u>A</u>ir − <u>C</u>omprehensive <u>O</u>rganic

3   <u>P</u>recursor <u>E</u>mission and <u>C</u>oncentration study) related to HONO chemistry and we provide a

4   detailed overview of its sources and sinks using a budget calculation for two measurement

5   heights, i.e. below and above a boreal forest canopy. We explicitly analyse additional source

6   terms, such as HONO emission by soil and the formation of HONO by photolysis of

7    $HNO_{3(ads)}$.

8

9 **2 Experimental**

10   The HUMPPA-COPEC-2010 was a comprehensively instrumented intensive field

11   measurement campaign, performed from 12 July until 12 August at the SMEAR II site

12   (Station for Measuring Ecosystem-Atmosphere Relation; 61.846°N, 24.295°E) located in the

13   Boreal forest in Hyytiälä (Williams et al., 2011).

14   HONO was measured using two Long Path Absorption Photometer instruments (LOPAP,

15   QUMA Elektronik & Analytik, Wuppertal, Germany). A detailed description of the

16   instrument has been given by Kleffmann et al. (2002) and Heland et al. (2001). Briefly, an

17   acidic solution of sulfanilamide is used to sample HONO with a stripping coil. HONO is

18   transformed rapidly into a diazonium salt, the precursor of diazotation, carried out in

19   sequence. The concentration of the azo dye formed is equivalent to the concentration of

20   HONO in the sampled air and is measured by a VIS-photometer. Artefacts due to wall

21   reactions are minimized in the LOPAP by using an external sampling unit where the

22   derivatization takes place, instead of using inlet lines. A short (L=1.5 cm) radiation shielded

23   glass inlet is the only instrument surface to which the sampling air is exposed to before

24   HONO is stripped in the first coil. The LOPAP uses two stripping coils in series. Hence,

25   potential interferences are accounted for by quantitatively sampling of HONO in the first coil

26   using a fast and specific reaction (Kleffmann et al., 2002; Heland et al., 2001). All

27   interferences are assumed to react in the same way in both coils and, therefore, the HONO

28   detection can be corrected using the measured "artefact HONO" in the second coil. The

29   background signal of the instrument was checked automatically for 30 minutes every four

30   hours using purified air. Consequently, all diurnal fluctuations of noise is monitored and

31   considered in the evaluation of the results. The comparison of both LOPAP instruments used

32   in this study has been described in detail by Sörgel et al. (2011b) and showed a good

agreement, within 12 % under dry conditions (no rain or fog). The inlets of the two instruments were positioned at about 1 m and 24 m above ground (canopy top height 20 to 21 m). Both instruments were operated with a response time of below 10 min and lower limit of detection ranging from 0.2 to 1.3 ppt during the campaign.

A laser induced fluorescence (LIF) instrument to measure the atmospheric concentration of the hydroxyl radical, OH, based on the fluorescence assay by gas expansion technique (FAGE) (Hens et al., 2014; Novelli et al., 2014) measured OH above the canopy at a height of about 24 m, while a chemical ionization mass spectrometer (CIMS; Petäjä et al., 2009) measured OH near to the ground at about 1 m. Lower detection limits of LIF and CIMS were about 9×10^5 molecules cm^{-3} and 5×10^4 molecules cm^{-3}, respectively. For a detailed description we refer to (Hens et al., 2014).

NO and NO_x were monitored by high resolution and high sensitivity chemiluminescence detectors, a TEI 42C TL (Thermo Fisher Scientific, US) with a limit of detection of about 0.1 ppb positioned at 4 m, and a modified (Hosaynali Beygi et al., 2011) CLD 790 SR with a detection limit of about 16 ppt (ECO-Physics, Switzerland) positioned at 24 m above ground. Both instruments use a blue light converter for efficient and selective transformation of NO_2 to NO. In addition ozone, O_3, was measured by a UV-absorption photometer above canopy.

The photolysis rates of NO_2 and O_3, $J(NO_2)$ and $J(O^1D)$, respectively, were measured using filter radiometers (Meteorologie consult, Königstein, Germany; Bohn et al., 2008). Two $J(NO_2)$ sensors were positioned at 2 m and 24 m above ground, and one $J(O^1D)$ sensor was placed at 24 m. Each measured the downwelling radiation. $J(HONO)$ was calculated from measured $J(NO_2)$ according to Trebs et al. (2009).

Relative humidity, temperature, wind direction, wind speed and other meteorological parameters were monitored routinely by the SMEAR II station (Junninen et al., 2009; http://www.atm.helsinki.fi/smartSMEAR/).

Evaluation of the boundary layer height was determined by radiosondes, measuring relative humidity, temperature, pressure and altitude. From this data vertical profiles of the potential temperature and the specific humidity were gained and hence the height and type of boundary layer have been inferred (Ouwersloot et al., 2012).

A sample from the O-horizon of soil was taken at 10 June 2012 at the measurement site and was measured under controlled conditions in the lab according to Oswald et al. (2013) to investigate NO and HONO emission fluxes from soil.

3   Results

Some instruments were not running continuously during the measurement period of HUMMPA-COPEC 2010 from 12 July to 12 August 2010.. Besides specific instrument malfunctions, several power disruptions caused by thunderstorms often interrupted the measurement. From 17 July until 5 August, the two LOPAP instruments were running about 30 % of the time simultaneously. The dataset of other measurements is close to complete for this period, except for the OH measurement above the canopy and the $J(NO_2)$ measurement below the canopy (see Fig. 1).

Besides a linear relationship found between OH measured at the forest floor and above canopy (Fig. 2), the exponential relationship of $J(NO_2)$ at 2 m above ground and $J(NO_2)$ at 24 m above ground was used to interpolate OH above the canopy and $J(NO_2)$ below the canopy to extend the data base for PSS calculations.

3.1   Diel variation of HONO

In the clean environment of Hyytiälä diurnal variations of HONO were observed with mean daytime concentrations of 6.6×10^8 molecules cm^{-3} (27 ppt) at 1 m height and 6.5×10^8 molecules cm^{-3} (26 ppt) at 24 m height and mean nighttime concentrations of 9.1×10^8 molecules cm^{-3} (37 ppt) at 1 m height and 9.2×10^8 molecules cm^{-3} (37 ppt) at 24 m. Maximum values reached 3.2×10^9 molecules cm^{-3} (132 ppt) at 1 m and 3.4×10^9 molecules cm^{-3} (138 ppt) at 24 m at 22:30 in the late evening of 2 August. The concentrations reached a minimum after a short and strong rain event in the morning of the 25 July with values below 2 ppt close to the detection limit. This emphasise that no uncorrected interferences occur in clean air , analogue to the observations of Sörgel et al. (2011a). The concentrations of HONO were calculated according to Eq. (5) by assuming a PSS, only valid for conditions with short photolytic lifetime of HONO. In agreement with Kleffmann et al. (2005) and Sörgel et al. (2011a) the box plots in Figure 3 obviously show that for both heights the calculated

concentrations are often more than one order of magnitude lower than the measured concentration of HONO. While the PSS calculation shows a peak in the morning (6:30) at 1 m height and around mid-morning (8:30) at 24 m height, the daytime measured HONO values peak at noon (11:30).

Sörgel et al. (2011a) stated that $[HONO]_{PSS}$ correlates best with measured [NO] and found neither a correlation to measured [OH] nor to measured J(HONO). The correlation between $[HONO]_{PSS}$ and [NO] was strong also in our data (Fig. 4). The reasonable correlation of $[HONO]_{PSS}$ to measured [NO] might serve as a proxy for $[HONO]_{PSS}$ in general, since the ratio seems to be quite constant.

$$\frac{[HONO]_{PSS}}{[NO]} = \frac{k_2[OH]}{J(HONO) + k_3[OH]} \cong 0.02 \tag{6}$$

J(HONO) at PSS shows values of about 2 orders of magnitude higher than k_2 or k_3 multiplied with the [OH]. Since OH formation is strongly linked to radiation (Rohrer and Berresheim, 2006), its concentration positively correlates with J(HONO). Therefore, NO drives the variability of the PSS.

3.2 HONO budget calculations

The two gas phase reactions (R2) and (R3) together with the photolysis fail to explain the observed HONO concentrations. The comparison of observed changes in HONO concentrations with calculated values considering further sources and sinks leads to a more complete understanding of HONO cycling.

$$\underbrace{\frac{\Delta[HONO]}{\Delta t}}_{observed} = \underbrace{Sources - Sinks}_{calculated\ budget} \tag{7}$$

If the calculated difference in sources and sinks equals the observed value, the budget would be closed. As mentioned before, normally this is not the case and an unknown source is missing, which can be calculated according to Su et al. (2008b) and Sörgel et al. (2011a) with the following equation:

$$P_{unknown} = \underbrace{\frac{\Delta[HONO]}{\Delta t}}_{observed} - \underbrace{k_2[NO][OH]}_{R2:\ P_{NO+OH}} - \underbrace{k_4^{dark}[NO_2]}_{R4:\ P_{het}} + \underbrace{J(HONO)[HONO]}_{R1:\ L_{phot}}$$

$$+ \underbrace{k_3[OH][HONO]}_{R3:\ L_{HONO+OH}} + \underbrace{\frac{v_{dep}}{h_{BL}}[HONO]}_{dry\ deposition:\ L_{dep}} \quad \underbrace{\pm T_h \pm T_v}_{\substack{horizontal\ and \\ vertical\ transport}} \qquad (8)$$

1   The resulting $P_{unknown}$ shows, that for most of the day there is still a large source missing (Fig.
2   5), at least for the period from 6:00 in the morning to 20:00 in the evening where HONO
3   lifetimes are below 30 min. This source is dominated by the photolytic loss of HONO that
4   forms the major sink for HONO and which exceeds the considered sources by far. Due to
5   generally low NO_2 values (below 2 ppb) the contribution of the dark heterogeneous NO_2
6   conversion (P_{het}) is very low, except for the early morning (before 7:00).

7   Not only the known sources seem to be small compared with the photolytic loss rate, also the
8   other sinks are negligible. E.g. with a deposition velocity for HONO of 2 cm s^{-1} (Harrison et
9   al., 1996; Su et al., 2008a), a mean daytime HONO concentration of 6.6 x 10^8 molecules cm^{-3}
10   and a typical boundary layer height at midday of about 1000 m, the deposition rate is 1.3 x
11   10^3 molecules cm^{-3} s^{-1}, i.e. 1.9 ppt/h and thus 1 to 2 orders of magnitude less than the
12   photolytic loss. The very low contribution of the dry deposition to HONO loss has already
13   been reported for other measurement campaigns (Su et al., 2008b; Sörgel et al., 2011a).

14   Horizontal transport, T_h, can strongly influence budget calculations in urban regions (Lee et
15   al., 2013). However, Hyytiälä is surrounded by uniform Boreal forest with up to 95 % of the
16   area within 5 km radius being forested, mostly by Scots pine and Spruce trees (Williams et
17   al., 2011) representing a homogenous fetch. Furthermore, with an average J(HONO) of about
18   6.7 x 10^{-4} s^{-1}, corresponding to a HONO lifetime of about 25 min and an average horizontal
19   wind speed of 2 m s^{-1} (maximum 7 m s^{-1}), direct emissions of HONO will be transported
20   about 3 km (maximum 10 km) within one lifetime. As most of the surrounding is covered by
21   forest and the next city Tampere, being nearly 50 km away there are no significant emission
22   sources within the fetch, thus horizontal advection of direct emissions will have little
23   influence on the HONO concentration during day. Therefore, the measurement site of
24   SMEAR II, with its homogeneous fetch is well suited to analyse the behaviour of $P_{unknown}$,
25   because all processes disturbing the analysis such as horizontal transport and direct emissions
26   can be neglected.

1   The contribution of vertical transport, T_v , to surface loss of HONO was estimated to be about

2   50 to 60 % (Wong et al., 2013), thus being the dominant loss process for HONO close to the

3   ground. Vertical mixing acts as a sink close to the surface and as an additional, yet

4   unaccounted source term at elevated levels. Hence, depending on the concentration gradient

5   of HONO and the ratio of photolysis, vertical transport can lead to reciprocal changes in

6   $P_{unknown}$ above canopy and below canopy when using the budget approach. Assuming the

7   unknown source is solely a ground source, $P_{unknown}$ is represented by T_v at elevated levels

8   ($P_{unknown} = T_v$). Nevertheless, without direct measurements of fluxes or the use of a chemistry

9   transport model, it is difficult to quantify T_v and its contribution remains uncertain. Without

10 explicitly considering T_v the budget approach is only reasonable for well mixed conditions

11 ($T_v = 0$).

12

13 ### 3.3   Tracing the missing source

14 ### 3.3.1 Influence of $J(NO_2)$ on $P_{unknown}$

15 Reactions (R5) and (R6-8) comprise several mechanisms of HONO formation from photolytic

16 dissociation of ortho-nitrophenols or light induced conversion of NO_2 on different reductive

17 surfaces, which are thought to be possible major sources for HONO during daytime

18 (Stemmler et al., 2006). The wavelength range for the proposed reactions is mostly covered

19 and well described by $J(NO_2)$. Therefore, a source corresponding to these reactions should

20 correlate to $J(NO_2)$ and especially the light induced conversion of NO_2 should correlate even

21 better with $P_{unknown}$ scaled to the NO_2 concentration (Fig. 6) (Sörgel et al., 2011a).

22 Scaling $P_{unknown}$ with the concentration of NO_2 on the ground leads to higher scattering of data

23 points, which might be caused by the higher noise levels of NO_2 data on ground. On the

24 contrary, the correlation above canopy is improved with similar scaling (figure 6 panels b and

25 d). The data points most affected belong to a period of rather cold and very clean conditions

26 with low NO_2 concentration of 1.6 to 2.9 x 10^9 molecules cm^{-3} (65 - 118 ppt) at the 23 July

27 (Williams et al., 2011). Since scaling $P_{unknown}$ above the canopy with corresponding NO_2

28 concentration increases the correlation with $J(NO_2)$, leads to the assumptions that either NO_2

29 plays a direct role in HONO formation or that in general NO_2 is a tracer for reactive nitrogen

30 (other potential HONO precursors) in the atmosphere. The fact that the correlation between

31 $P_{unknown}$ and $J(NO_2)$ below the canopy descends by scaling $P_{unknown}$ with NO_2 concentrations

can be either due to data scattering as mentioned above, due to HONO deposition on the forest floor (Sörgel et al., 2014) or due to different pathways of HONO and NO_2 formation below canopy. NO_2 below canopy is formed by shifted PSS below canopy and additional NO soil emissions oxidized by O_3 (Rummel et al., 2002). Opposed, due to low OH and NO values below canopy, the shift in the $[HONO]_{PSS}$ by reduced radiation below canopy has minor influence on HONO values (Fig. 3).

Since measurements of ortho-nitrophenols were not available, it is not possible to rule out that photolytic conversion of these compounds is a possible pathway. . However, from Eq. 3 we estimate that the concentration of o-NPs has to exceed the concentration of HONO by a factor of about 70 in order to compensate the photolytic loss of HONO. Taking the average daytime mixing ratio of HONO above canopy, the resulting mixing ratio of o-NPs would be about 1.8 ppb. Based on earlier studies (Bejan et al., 2006; Kourtchev et al., 2013), the concentration in clean environment such as Hyytiälä should be much lower and, thus, insignificant for HONO formation.

Another possible HONO source that depends on $J(NO_2)$ is the photolytic activation of organic surface reactants (R6-8) to reduce NO_2 and form HONO (Stemmler et al., 2006). But as previously mentioned, due to the lack of in-situ measurements of all quantities, this contribution could not be calculated. Obviously, it is likely that humic acids or similar compounds occur in the highly organic surrounding of the Boreal Forest. A strong hint on such a source might be the merging effect on the correlation of the $P_{unknown}$ with $J(NO_2)$ by scaling with the concentration of NO_2 above the canopy.

As radical formation is driven by sunlight as well, the recently proposed reaction of the HO_2-water complex with NO_2 as a potential HONO source (Li et al., 2014) might be correlated to radiation as well. The contribution of this source was estimated using the measured HO_2 concentration, a water vapour mixing ratio of 1.5 % (Hens et al. 2014) and the equilibrium constant (Sander et al., 2011) to calculate the complex formation. All calculations were made using 298 K and 1013 hPa as standard conditions. Hence, about 20 % of the HO_2 is complexed to water. The related HONO formation was calculated by using the rate constant (298 K, 1013 hPa) of the reaction of HO_2 and NO_2 without water according to Atkinson et al. (2004) and a 20 % enhancement of the reaction rate due to water vapour for conditions in the lower atmosphere (Sander and Peterson, 1984). Assuming a 100 % yield of HONO formation from the reaction of the complexed HO_2 with NO_2, as postulated by Li et al. (2014), the

1 HONO formation by this source is a factor three to ten higher than the required unknown

2 source. Li et al (2014) reproduced their unknown HONO source by including these reactions.

3 However, their required HONO source was about a factor of four higher (~ 600 ppt h^{-1}) than

4 in our case at comparable NO_2 ($0.5 - 1$ ppb) and HO_2 ($5 - 10 \times 10^8$ molec cm^{-3}) levels.

5 Additionally, the HONO to NO_x ratios were normally below 10 % in our study, while they

6 were relatively high ($\sim 10 - 30$ %) in the study of Li et al. (2014). Consequently, our results

7 indicate a NO_x to HONO conversion that is smaller than in Li et al (2014). Using the upper

8 limit rate constant for HONO formation in the reaction of NO_2 and HO_2 without water given

9 by Tyndall et al. (1995), this reaction did not lead to substantial HONO formation (factor 100

10 to 200 below the required values), which is consistent with earlier findings (Kleffmann,

11 2007). Hence, the contribution of this source to HONO formation in our study will depend on

12 the reaction mechanism (i.e. the yield of HONO) which is still unclear and needs to be further

13 investigated in laboratory studies.

14 ### 3.3.2 Indirect influence of $J(NO_2)$ on $P_{unknown}$

15 Besides the activation or the photolytic reaction of molecules by $J(NO_2)$, the radiation

16 influences also other parameters. One of these is the temperature of soil. The temperature of

17 soil surface changes stronger and faster than in deeper layers of soil and is driven by radiative

18 heating and cooling. Nitrification and denitrification by microorganisms takes place at the

19 uppermost layer of soil and produces reactive nitrogen gases (Conrad, 1996). The rate of

20 reactive nitrogen formation depends on many parameters like soil water content (SWC), pH,

21 nutrient availability and, important in this context, the temperature of soil (Skopp et al., 1990;

22 Oswald et al., 2013). Therefore, radiation can accelerate the formation of HONO by soil.

23 Since we did not measure the potential emission of HONO by soil in the field, a soil sample

24 was taken afterwards and measured in the laboratory under controlled conditions according to

25 Oswald et al. (2013). Concentrations of nutrients were quite low with ammonium being (1.60

26 ± 0.56) mg kg^{-1} N-NH_4^+, while NO_3^- and NO_2^- were not measureable (below LOD, i.e. 2 mg

27 kg^{-1} N-NO_3^- and 0.07 mg kg^{-1} N-NO_2^-). This is in good agreement with Korhonen et al.

28 (2013), who found that the measurement site of Hyytiälä provides nutrient poor soils with

29 NH_4^+ as the dominant inorganic nitrogen compound in the extract of soil organic layer (0.31

30 kg ha^{-1} N-NH_4^+) and the first 30 cm of mineral soil, while NO_3^- forms only 0.6 % of it. The

31 soil pH was very low with a value of about 3.0. The measurement of the soil sample showed

32 no significant emission fluxes of HONO being below the limit of detection (0.08 ng m^{-2} s^{-1} =

1    $0.288 \ \mu g \ m^{-2} \ h^{-1}$) and emission fluxes of NO scattering around the limit of detection (1 ng m^{-2}

2   s^{-1} = 3.6 $\mu g \ m^{-2} \ h^{-1}$). This is in good agreement with Oswald et al. (2013) and Maljanen et al.

3   (2013), who both found that acidic forest soils tend to low emission fluxes of HONO.

4   Maljanen et al. (2013) measured a maximum HONO flux of about 2 $\mu g \ m^{-2} \ h^{-1}$ in terms of N.

5   This would equal a source-strength of 7.1 x 10^3 molecules cm^{-3} s^{-1} (1 ppt h^{-1}) considering a

6   boundary layer height of 1000 m and hence is negligible. The laboratory measurements of soil

7   samples represent potential HONO emission fluxes as HONO can simultaneously be taken up

8   by soil (Donaldson et al., 2014) or deposited to soil and reemitted as proposed by

9   VandenBoer et al. (2013). In addition to emissions from the soil surface, the evaporation of

10   dew can release HONO (He et al., 2006) also enhancing HONO fluxes in the early morning ,

11   when temperatures increase.

12   ### 3.3.3 HONO formation by nitric acid photolysis

13   Adsorbed HNO$_3$ on humid surfaces (R9) seems to be more rapidly photolyzed than HNO$_3$ in

14   the gas phase or in aqueous solution (Zhou et al., 2003; Abida et al., 2012). Therefore, leaves

15   and needles loaded with nitric acid could be a major source of HONO in clean environments

16   (Zhou et al., 2011). This mechanism has also been postulated as significant for the Boreal

17   forest by Raivonen et al. (2006) to explain light induced NO$_y$ (NO, NO$_2$, HONO, HNO$_3$,

18   peroxy acyl nitrate) emissions. To estimate the strength of this source we used a constant

19   surface loading of HNO$_3$ of (8.3 ± 3.1) x 10^{-5} mol m^{-2}, which is close to one monolayer

20   coverage (Zhou et al., 2011). The site investigated by Zhou et al. (2011) (PROPHET) was

21   located in a mixed forest (~ 45° N), whereas the SMEAR II station is located in a boreal forest

22   (~ 62 ° N) with the main tree species being scots pine. Nevertheless, both sites are rural

23   forested sites with low local pollution and low NO$_x$ concentrations (Kulmala et al., 2000;

24   Carroll et al., 2001). Therefore, we assume that the values derived by Zhou and co-workers

25   (Zhou et al., 2011; Zhou et al., 2003) constitute a reasonable estimate for the conditions at the

26   SMEAR site. The gas phase photolysis frequency for HNO$_3$ was parameterized using J(NO$_2$)

27   and J(O^{1}D) (Sander et al., 2011). By adsorbing to the surface the absorption cross-sections of

28   HNO$_3$ increases (Zhu et al., 2010; Abida et al., 2012), which is typically considered by the

29   use of an empirical enhancement factor for natural systems (Zhou et al., 2011; Li et al., 2012).

30   According to the similar environment in the study of Zhou and co-workers, we used their

31   enhancement factor of 43 for Figure 7 (Zhou et al., 2003; Zhou et al., 2011).

1   The photolysis rate of surface adsorbed HNO_3 needs to be more than 400 times enhanced

2   compared to the photolysis in gas phase to explain $P_{unknown}$ of HONO (Fig. 7), which is still

3   within the estimated range (e.g. Zhu et al., 2008; Zhu et al., 2010¸Baergen and Donaldson,

4   2013). Nevertheless, the enhancement factor given by Zhou et al. (2011) is the only reported

5   value on the HONO formation rate (instead of HNO_3 photolysis rate) with respect to HNO_3

6   photolysis on natural surfaces. The error of $P_{HNO3(ads)}$ was calculated by using the standard

7   error of the surface loading of HNO_3 (Zhou et al., 2011). $J(HNO_3)$ constitutes the only

8   variable of $P_{HNO3(ads)}$ and is closely correlated to $J(NO_2)$ and $J(O^1D)$. This leads to a similar

9   correlation of $P_{unknown}$ with $P_{HNO3(ads)}$, like seen before with $J(NO_2)$ (Fig. 6). An additional

10   correlation might derive from the mechanism of HNO_3 photolysis, which is not fully

11   understood by now. Zhou et al. (2011) proposed that formed NO_2 during HNO_3 photolysis

12   reacts further with organics on the surface to form HONO (R6) as proposed by Stemmler et

13   al. (2006).

14

15   ## 3.4   Direct comparison of $P_{unknown}$ determined for two different heights

16   The ratio of $J(NO_2)$ at 24 m to $J(NO_2)$ at 2 m tracks the ratio of direct and diffuse radiation

17   penetrating the canopy. In the early morning the ratio increases, due to increasing direct

18   sunlight at the upper height. With the rising sun more direct sunlight penetrates the canopy

19   and a rather constant ratio develops which seems to be influenced by light patches. The ratio

20   of $P_{unknown}$ at 24 m to $P_{unknown}$ at 1 m during daytime is mainly above 1, except for the first

21   value where $P_{unknown}$ at both heights were still negative (Fig. 5). It strongly decreases from

22   values above 4 in the morning hours before it gets more stable with values around 2, but still

23   decreases until 2 hours after reaching the minimum of solar zenith angle (~43°). This diel

24   pattern can be explained by a combination of two processes; the change of the photolysis

25   frequency and the change of the concentration gradient (Fig. 8 a). The product of both, the

26   concentration and the photolysis frequency equals the photolytic loss rate, L_{phot}, which is the

27   unbalanced sink that determines $P_{unknown}$ (see Fig.5, Fig. 8 panels b and c). This is at least

28   valid from 8:30 to 17:30 where the contribution of other source and sink terms is less than 20

29   %. The HONO concentrations above the canopy are higher than below the canopy in the

30   morning (values over unity in Fig 8a). The gradients vary around zero from late morning to

31   noon and in the afternoon the concentrations below the canopy are higher. This closely

32   resembles the pattern found by Sörgel et al. (2011b) for a different forest ecosystem and

16

might therefore be typical for forests in general. Sörgel et al. (2011b) showed that this could be attributed to different sources and sinks and the extent of the vertical exchange between the forest and the atmosphere above. However, the variability of the ratios is smallest at minimum solar zenith angle, which is the maximum of J(HONO). In a strict sense this is the only period where the budget could be used for the determination of $P_{unknown}$ as the assumptions like well mixed conditions (i.e. no concentration gradients), stationarity due to low lifetime of HONO and potentially establishment of a PSS are fulfilled. During this period it could be questioned if a budget below canopy makes sense as the portion below canopy where J(HONO) and thus L_{phot} is reduced is very small compared to the whole boundary layer and recombination of NO and OH below canopy has been found to play a minor role (section 3.2).

Impressively, $P_{unknown}$ correlates much better with L_{phot} (Fig. 8 b and c) than with $J(NO_2)$ or with the ratio of $J(NO_2)$ to concentration of NO_2 (Fig. 6). This correlation (Fig. 8 b and c) is not disturbed by any environmental condition, like the different regimes of stressed and normal Boreal and even more astonishing it is not disturbed by the wild fire pollution plumes transported from Russia (Nölscher et al., 2012). The almost perfect correlation of $P_{unknown}$ with L_{phot} is caused by the low contribution to the budget of all other processes (sources and sinks) considered so far. Even including the parameterized HNO_3 photolysis (Sec. 3.4.3) would not change much as it is only around 10 % of $P_{unknown}$. Therefore, the unknown source is a process that exactly balances HONO photolysis or the sink itself is erroneous. Nevertheless, this unbalanced photolysis term ($P_{unknown}$) has been found by applying different techniques for HONO detection such as LOPAP (e.g., Kleffmann et al., 2005; Sörgel et al., 2011a), denuder (Acker et al., 2006), differential optical absorption spectroscopy (Alicke et al., 2002; Wong et al., 2012) and recently by using chemical ionization mass spectroscopy (VandenBoer et al., 2013). Consequently, the unknown HONO source is very unlikely to be caused by an instruments artefact. Additionally, recent flux measurements reported strong daytime upward fluxes of HONO (Zhou et al., 2011, Ren et al., 2011), thus confirming a ground source of HONO.

4 Conclusion

Concentrations of HONO during daytime exceeded the expected values calculated by the PSS on average by a factor of about 20 and, thus, lead to an imbalanced budget above and below canopy. An additional yet unknown source is required to balance the budget. However,

photolysis of ortho-nitrophenols is likely of minor importance under the clean environment of the Boreal Forest. A laboratory measurement of a soil sample in a dynamic chamber shows that direct soil emissions of HONO are insignificant for the measurement site in the Boreal Forest, featuring low soil nutrient content and low soil pH. However, the photolytically active radiation has a major influence on the budget of HONO, since the missing source resembles the photolytic daytime loss of HONO. It was not possible to clearly identify the most important source term, but a tendency for a possible coupling of different processes is most likely. For instance, the photolytic dissociation of HNO_3 adsorbed on humid surfaces and the conversion of NO_2 on photolytically activated surfaces, like humic acids, might occur simultaneously. However, the almost perfect correlation of $P_{unknown}$ with L_{phot} is caused by the low contribution of the considered processes to the budget and, hence, the unknown source is a process that exactly balances HONO photolysis. Further field investigations are needed to understand daytime HONO chemistry and its implication for the budget. Especially the role of vertical mixing needs to be analysed in more detail.

Acknowledgements

References

Abida, O., Du, J., and Zhu, L.: Investigation of the photolysis of the surface-adsorbed HNO_3 by combining laser photolysis with Brewster angle cavity ring-down spectroscopy, Chem. Phys. Lett., 534, 77-82, 10.1016/j.cplett.2012.03.034, 2012.

Acker, K., Moller, D., Wieprecht, W., Meixner, F. X., Bohn, B., Gilge, S., Plass-Dülmer, C., and Berresheim, H.: Strong daytime production of OH from HNO_2 at a rural mountain site, Geophysical Research Letters, 33, L02809, doi:02810.01029/02005GL024643, 2006.

Alicke, B., Platt, U., and Stutz, J.: Impact of nitrous acid photolysis on the total hydroxyl radical budget during the Limitation of Oxidant Production/Pianura Padana Produzione di Ozono study in Milan, J. Geophys. Res., 107, LOP9-1-LOP9-LOP9-17, 10.1029/2000jd000075, 2002.

Atkinson, R., Baulch, D. L., Cox, R. A., Crowley, J. N., Hampson, R. F., Hynes, R. G., Jenkin, M. E., Rossi, M. J., and Troe, J.: Evaluated kinetic and photochemical data for atmospheric chemistry: Volume I - gas phase reactions of O_x, HO_x, NO_x and SO_x species, Atmospheric Chemistry and Physics, 4, 1461-1738, 2004.

Aubin, D. G., and Abbatt, J. P. D.: Interaction of NO_2 with hydrocarbon soot: Focus on HONO yield, surface modification, and mechanism, Journal of Physical Chemistry A, 111, 6263-6273, 2007.

Baergen, A. M., and Donaldson, D. J.: Photochemical Renoxification of Nitric Acid on Real Urban Grime, Environmental Science & Technology, 47, 815-820, 10.1021/es3037862, 2013.

Bejan, I., Abd El Aal, Y., Barnes, I., Benter, T., Bohn, B., Wiesen, P., and Kleffmann, J.: The photolysis of ortho-nitrophenols: a new gas phase source of HONO, Physical Chemistry Chemical Physics, 8, 2028-2035, 2006.

Bohn, B., Corlett, G. K., Gillmann, M., Sanghavi, S., Stange, G., Tensing, E., Vrekoussis, M., Bloss, W. J., Clapp, L. J., Kortner, M., Dorn, H. P., Monks, P. S., Platt, U., Plass-Dülmer, C., Mihalopoulos, N., Heard, D. E., Clemitshaw, K. C., Meixner, F. X., Prevot, A. S. H., and Schmitt, R.: Photolysis frequency measurement techniques: results of a comparison within the ACCENT project, Atmospheric Chemistry and Physics, 8, 5373-5391, 2008.

Carroll, M. A., Bertman, S. B., and Shepson, P. B.: Overview of the Program for Research on Oxidants: PHotochemistry, Emissions, and Transport (PROPHET) summer 1998 measurements intensive, J. Geophys. Res., 106, 24 275–24 288, 2001.

Conrad, R.: Soil microorganisms as controllers of atmospheric trace gases (H_2, CO, CH_4, OCS, N_2O, and NO), Microbiological Reviews, 60, 609-+, 1996.

De Jesus Medeiros, D., and Pimentel, A. S.: New insights in the atmospheric HONO formation: New pathways for N_2O_4 isomerization and NO_2 dimerization in the presence of water, Journal of Physical Chemistry A, 115, 6357-6365, 2011.

Donaldson, M. A., Berke, A. E., and Raff, J. D.: Uptake of Gas Phase Nitrous Acid onto Boundary Layer Soil Surfaces, Environmental Science & Technology, 48, 375-383, 10.1021/es404156a, 2014.

Elshorbany, Y. F., Steil, B., Brühl, C., and Lelieveld, J.: Impact of HONO on global atmospheric chemistry calculated with an empirical parameterization in the EMAC model, Atmospheric Chemistry and Physics, 12, 9977-10000, 10.5194/acp-12-9977-2012, 2012.

Finlayson-Pitts, B. J., Wingen, L. M., Sumner, A. L., Syomin, D., and Ramazan, K. A.: The heterogeneous hydrolysis of NO_2 in laboratory systems and in outdoor and indoor

atmospheres: An integrated mechanism, Physical Chemistry Chemical Physics, 5, 223-242, 10.1039/b208564j, 2003.

Goodman, A. L., Bernard, E. T., and Grassian, V. H.: Spectroscopic Study of Nitric Acid and Water Adsorption on Oxide Particles: Enhanced Nitric Acid Uptake Kinetics in the Presence of Adsorbed Water, The Journal of Physical Chemistry A, 105, 6443-6457, 10.1021/jp003722l, 2001.

Harrison, R. M., Peak, J. D., and Collins, G. M.: Tropospheric cycle of nitrous acid, Journal of Geophysical Research-Atmospheres, 101, 14429-14439, 1996.

He, Y., Zhou, X., Hou, J., Gao, H., and Bertman, S. B.: Importance of dew in controlling the air-surface exchange of HONO in rural forested environments, Geophysical Research Letters, 33, L02813, 10.1029/2005GL024348, 2006.

Heland, J., Kleffmann, J., Kurtenbach, R., and Wiesen, P.: A new instrument to measure gaseous nitrous acid (HONO) in the atmosphere, Environmental Science & Technology, 35, 3207-3212, 10.1021/es000303t, 2001.

Hens, K., Novelli, A., Martinez, M., Auld, J., Axinte, R., Bohn, B., Fischer, H., Keronen, P., Kubistin, D., Nölscher, A. C., Oswald, R., Paasonen, P., Petäjä, T., Regelin, E., Sander, R., Sinha, V., Sipilä, M., Taraborrelli, D., Tatum Ernest, C., Williams, J., Lelieveld, J., and Harder, H.: Observation and modelling of HO_x radicals in a boreal forest, Atmos. Chem. Phys. Discuss., 13, 28561-28629, 10.5194/acpd-13-28561-2013, 2013.

Hosaynali Beygi, Z., Fischer, H., Harder, H. D., Martinez, M., Sander, R., Williams, J., Brookes, D. M., Monks, P. S., and Lelieveld, J.: Oxidation photochemistry in the Southern Atlantic boundary layer: unexpected deviations of photochemical steady state, Atmos. Chem. Phys., 11, 8497-8513, 10.5194/acp-11-8497-2011, 2011.

Junninen, H., Lauri, A., Keronen, P., Aalto, P., Hiltunen, V., Hari, P., and Kulmala, M.: Smart-SMEAR: on-line data exploration and visualization tool for SMEAR stations., Boreal Environ. Res., 14, 447-457, 2009.

Kleffmann, J., Heland, J., Kurtenbach, R., Lörzer, J., and Wiesen, P.: A new instrument (LOPAP) for the detection of nitrous acid (HONO), Environmental Science and Pollution Research, 48-54, 2002.

Kleffmann, J., Kurtenbach, R., Lörzer, J., Wiesen, P., Kalthoff, N., Vogel, B., and Vogel, H.: Measured and simulated vertical profiles of nitrous acid - Part I: Field measurements, Atmospheric Environment, 37, 2949-2955, 10.1016/s1352-2310(03)00242-5, 2003.

Kleffmann, J., Gavriloaiei, T., Hofzumahaus, A., Holland, F., Koppmann, R., Rupp, L., Schlosser, E., Siese, M., and Wahner, A.: Daytime formation of nitrous acid: A major source of OH radicals in a forest, Geophysical Research Letters, 32, 2005.

Kleffmann, J.: Daytime sources of nitrous acid (HONO) in the atmospheric boundary layer, ChemPhysChem, 8, 1137-1144, 2007.

Korhonen, J. F. J., Pihlatie, M., Pumpanen, J., Aaltonen, H., Hari, P., Levula, J., Kieloaho, A. J., Nikinmaa, E., Vesala, T., and Ilvesniemi, H.: Nitrogen balance of a boreal Scots pine forest, Biogeosciences, 10, 1083-1095, 10.5194/bg-10-1083-2013, 2013.

Kourtchev, I., Fuller, S., Aalto, J., Ruuskanen, T. M., McLeod, M. W., Maenhaut, W., Jones, R., Kulmala, M., and Kalberer, M.: Molecular Composition of Boreal Forest Aerosol from Hyytiala, Finland, Using Ultrahigh Resolution Mass Spectrometry, Environmental Science & Technology, 47, 4069-4079, 10.1021/es3051636, 2013.

Kraus, A., and Hofzumahaus, A.: Field measurements of atmospheric photolysis frequencies for O_3, NO_2, HCHO, CH_3CHO, H_2O_2, and HONO by UV spectroradiometry, J. Atmos. Chem., 31, 161-180, 1998.

Kubota, M., and Asami, T.: Volatilization of nitrous-acid from upland soils, Soil Sci. Plant Nutr., 31, 27-34, 1985.

Kulmala, M., Rannik, U., Pirjola, L., Dal Maso, M., Karimäki, J., Asmi, A., Jäppinen, A., Karhu, V., Korhonen, H., Malvikko, S. P., Puustinen, A., Raittila, J., Romakkaniemi, S., Suni, T., Yli-Koivisto, S., Paatero, J., Hari, P. and Vesala, T.: Characterization of atmospheric trace gas and aerosol concentrations at forest sites in southern and northern Finland using back trajectories, Boreal Environ. Res., 5, 315–336, 2000.

Lammel, G., and Cape, J. N.: Nitrous acid and nitrite in the atmosphere, Chemical Society Reviews, 25, 361-369, 1996.

Lee, B. H., Wood, E. C., Herndon, S. C., Lefer, B. L., Luke, W. T., Brune, W. H., Nelson, D. D., Zahniser, M. S., and Munger, J. W.: Urban measurements of atmospheric nitrous acid: A caveat on the interpretation of the HONO photostationary state, Journal of Geophysical Research: Atmospheres, 118, 2013JD020341, 10.1002/2013JD020341, 2013.

Li, X., Brauers, T., Haseler, R., Bohn, B., Fuchs, H., Hofzumahaus, A., Holland, F., Lou, S., Lu, K. D., Rohrer, F., Hu, M., Zeng, L. M., Zhang, Y. H., Garland, R. M., Su, H., Nowak, A., Wiedensohler, A., Takegawa, N., Shao, M., and Wahner, A.: Exploring the atmospheric chemistry of nitrous acid (HONO) at a rural site in Southern China, Atmospheric Chemistry and Physics, 12, 1497-1513, 10.5194/acp-12-1497-2012, 2012.

Maljanen, M., Yli-Pirilä, P., Hytönen, J., Joutsensaari, J., and Martikainen, P. J.: Acidic northern soils as sources of atmospheric nitrous acid (HONO), Soil Biology and Biochemistry, 67, 94-97, http://dx.doi.org/10.1016/j.soilbio.2013.08.013, 2013.

Monge, M. E., D'Anna, B., Mazri, L., Giroir-Fendler, A., Ammann, M., Donaldson, D. J., and George, C.: Light changes the atmospheric reactivity of soot, Proc. Natl. Acad. Sci. U. S. A., 107, 6605-6609, 10.1073/pnas.0908341107, 2010.

Nölscher, A. C., Williams, J., Sinha, V., Custer, T., Song, W., Johnson, A. M., Axinte, R., Bozem, H., Fischer, H., Pouvesle, N., Phillips, G., Crowley, J. N., Rantala, P., Rinne, J., Kulmala, M., Gonzales, D., Valverde-Canossa, J., Vogel, A., Hoffmann, T., Ouwersloot, H. G., de Arellano, J. V. G., and Lelieveld, J.: Summertime total OH reactivity measurements from boreal forest during HUMPPA-COPEC 2010, Atmospheric Chemistry and Physics, 12, 8257-8270, 10.5194/acp-12-8257-2012, 2012.

Novelli, A., Hens, K., Tatum Ernest, C., Kubistin, D., Regelin, E., Elste, T., Plass-Dülmer, C., Martinez, M., Lelieveld, J., and Harder, H.: Characterisation of an inlet pre-injector laser induced fluorescence instrument for the measurement of ambient hydroxyl radicals, Atmos. Meas. Tech. Discuss., 7, 819-858, 10.5194/amtd-7-819-2014, 2014.

Oswald, R., Behrendt, T., Ermel, M., Wu, D., Su, H., Cheng, Y., Breuninger, C., Moravek, A., Mougin, E., Delon, C., Loubet, B., Pommerening-Röser, A., Sorgel, M., Pöschl, U., Hoffmann, T., Andreae, M. O., Meixner, F. X., and Trebs, I.: HONO Emissions from Soil Bacteria as a Major Source of Atmospheric Reactive Nitrogen, Science, 341, 1233-1235, 10.1126/science.1242266, 2013.

Ouwersloot, H. G., de Arellano, J. V. G., Nölscher, A. C., Krol, M. C., Ganzeveld, L. N., Breitenberger, C., Mammarella, I., Williams, J., and Lelieveld, J.: Characterization of a boreal convective boundary layer and its impact on atmospheric chemistry during HUMPPA-COPEC-2010, Atmospheric Chemistry and Physics, 12, 9335-9353, 10.5194/acp-12-9335-2012, 2012.

Park, J. Y., and Lee, Y. N.: Solubility and decomposition kinetics of nitrous-acid in aqueous-solution, J. Phys. Chem., 92, 6294-6302, 10.1021/j100333a025, 1988.

Perner, D., and Platt, U.: Detection of nitrous-acid in the atmosphere by differential optical-absorption, Geophysical Research Letters, 6, 917-920, 10.1029/GL006i012p00917, 1979.

Petäjä, T., Mauldin Iii, R. L., Kosciuch, E., McGrath, J., Nieminen, T., Paasonen, P., Boy, M., Adamov, A., Kotiaho, T., and Kulmala, M.: Sulfuric acid and OH concentrations in a boreal forest site, Atmos. Chem. Phys., 9, 7435-7448, 10.5194/acp-9-7435-2009, 2009.

Raivonen, M., Bonn, B., Sanz, M. J., Vesala, T., Kulmala, M., and Hari, P.: UV-induced NOy emissions from Scots pine: Could they originate from photolysis of deposited HNO3?, Atmospheric Environment, 40, 6201-6213, 10.1016/j.atmosenv.2006.03.063, 2006.

Ramazan, K. A., Syomin, D., and Finlayson-Pitts, B. J.: The photochemical production of HONO during the heterogeneous hydrolysis of NO_2, Physical Chemistry Chemical Physics, 6, 3836-3843, 2004.

Ren, X., Sanders, J. E., Rajendran, A., Weber, R. J., Goldstein, A. H., Pusede, S. E., Browne, E. C., Min, K. E., and Cohen, R. C.: A relaxed eddy accumulation system for measuring vertical fluxes of nitrous acid, Atmospheric Measurement Techniques, 4, 2093-2103, 10.5194/amt-4-2093-2011, 2011.

Rohrer, F., and Berresheim, H.: Strong correlation between levels of tropospheric hydroxyl radicals and solar ultraviolet radiation, Nature, 442, 184-187, 10.1038/nature04924, 2006.

Rummel, U., Ammann, C., Gut, A., Meixner, F. X., and Andreae, M. O.: Eddy covariance measurements of nitric oxide flux within an Amazonian rain forest, J. Geophys. Res., 107, LBA17-11-19, 10.1029/2601jd000520, 2002.

Sander, S. P., Abbatt, J. P. D., Barker, J. R., Burkholder, J. B., Friedl, R. R., Golden, D. M., Huie, R. E., Kolb, C. E., Kurylo, M. J., Moortgat, G. K., Orkin, V. L., and Wine, P. H.: Chemical Kinetics and Photochemical Data for Use in Atmospheric Studies, Evaluation No. 17, in: JPL Publication 10-6, Jet Propulsion Laboratory, Pasadena, 2011.

Sander, S. P. and Peterson, M.: Kinetics of the reaction $HO_2 + NO_2 + M => HO_2NO_2 + M$, J. Phys. Chem., 88, 1566-1571, 1984.

Skopp, J., Jawson, M. D., and Doran, J. W.: Steady-state aerobic microbial activity as a function of soil-water content, Soil Science Society of America Journal, 54, 1619-1625, 1990.

Sörgel, M., Regelin, E., Bozem, H., Diesch, J. M., Drewnick, F., Fischer, H., Harder, H., Held, A., Hosaynali-Beygi, Z., Martinez, M., and Zetzsch, C.: Quantification of the unknown HONO daytime source and its relation to NO_2, Atmospheric Chemistry and Physics, 11, 10433-10447, 10.5194/acp-11-10433-2011, 2011a.

Sörgel, M., Trebs, I., Serafimovich, A., Moravek, A., Held, A., and Zetzsch, C.: Simultaneous HONO measurements in and above a forest canopy: influence of turbulent exchange on mixing ratio differences, Atmospheric Chemistry and Physics, 11, 841-855, 10.5194/acp-11-841-2011, 2011b.

Sörgel, M., Wu, D., Trebs, I., and Held, A.: A comparison of measured HONO uptake and release with calculated source strengths in a heterogeneous forest environment., submitted to Atmos. Chem. Phys. Discuss., 2014.

Stemmler, K., Ammann, M., Donders, C., Kleffmann, J., and George, C.: Photosensitized reduction of nitrogen dioxide on humic acid as a source of nitrous acid, Nature, 440, 195-198, 2006.

Stemmler, K., Ndour, M., Elshorbany, Y., Kleffmann, J., D'Anna, B., George, C., Bohn, B., and Ammann, M.: Light induced conversion of nitrogen dioxide into nitrous acid on

submicron humic acid aerosol, Atmospheric Chemistry and Physics, 7, 4237-4248, 2007.

Su, H., Cheng, Y. F., Cheng, P., Zhang, Y. H., Dong, S., Zeng, L. M., Wang, X., Slanina, J., Shao, M., and Wiedensohler, A.: Observation of nighttime nitrous acid (HONO) formation at a non-urban site during PRIDE-PRD2004 in China, Atmospheric Environment, 42, 6219-6232, 10.1016/j.atmosenv.2008.04.006, 2008a.

Su, H., Cheng, Y. F., Shao, M., Gao, D. F., Yu, Z. Y., Zeng, L. M., Slanina, J., Zhang, Y. H., and Wiedensohler, A.: Nitrous acid (HONO) and its daytime sources at a rural site during the 2004 PRIDE-PRD experiment in China, Journal of Geophysical Research-Atmospheres, 113, 10.1029/2007jd009060, 2008b.

Su, H., Cheng, Y., Oswald, R., Behrendt, T., Trebs, I., Meixner, F. X., Andreae, M. O., Cheng, P., Zhang, Y., and Pöschl, U.: Soil Nitrite as a Source of Atmospheric HONO and OH Radicals, Science, 333, 1616-1618, 10.1126/science.1207687, 2011.

Trebs, I., Bohn, B., Ammann, C., Rummel, U., Blumthaler, M., Königstedt, R., Meixner, F. X., Fan, S., and Andreae, M. O.: Relationship between the NO_2 photolysis frequency and the solar global irradiance, Atmospheric Measurement Techniques, 2, 725-739, 2009.

Twigg, M. M., House, E., Thomas, R., Whitehead, J., Phillips, G. J., Famulari, D., Fowler, D., Gallagher, M. W., Cape, J. N., Sutton, M. A., and Nemitz, E.: Surface/atmosphere exchange and chemical interactions of reactive nitrogen compounds above a manured grassland, Agricultural and Forest Meteorology, 151, 1488-1503, 10.1016/j.agrformet.2011.06.005, 2011.

Tyndall, G. S., Orlando, J. J., and Calvert, J. G.: Upper limit for the rate coefficient for the reaction HO2+NO2 => HONO + O2, Environ. Sci. Technol., 29, 202–206, 1995.

VandenBoer, T. C., Brown, S. S., Murphy, J. G., Keene, W. C., Young, C. J., Pszenny, A. A. P., Kim, S., Warneke, C., de Gouw, J. A., Maben, J. R., Wagner, N. L., Riedel, T. P., Thornton, J. A., Wolfe, D. E., Dubé, W. P., Öztürk, F., Brock, C. A., Grossberg, N., Lefer, B., Lerner, B., Middlebrook, A. M., and Roberts, J. M.: Understanding the role of the ground surface in HONO vertical structure: High resolution vertical profiles during NACHTT-11, Journal of Geophysical Research: Atmospheres, 118, 10,155-110,171, 10.1002/jgrd.50721, 2013.

Williams, J., Crowley, J., Fischer, H., Harder, H., Martinez, M., Petaja, T., Rinne, J., Back, J., Boy, M., Dal Maso, M., Hakala, J., Kajos, M., Keronen, P., Rantala, P., Aalto, J., Aaltonen, H., Paatero, J., Vesala, T., Hakola, H., Levula, J., Pohja, T., Herrmann, F., Auld, J., Mesarchaki, E., Song, W., Yassaa, N., Nolscher, A., Johnson, A. M., Custer, T., Sinha, V., Thieser, J., Pouvesle, N., Taraborrelli, D., Tang, M. J., Bozem, H., Hosaynali-Beygi, Z., Axinte, R., Oswald, R., Novelli, A., Kubistin, D., Hens, K., Javed, U., Trawny, K., Breitenberger, C., Hidalgo, P. J., Ebben, C. J., Geiger, F. M., Corrigan, A. L., Russell, L. M., Ouwersloot, H. G., de Arellano, J. V. G., Ganzeveld, L., Vogel, A., Beck, M., Bayerle, A., Kampf, C. J., Bertelmann, M., Kollner, F., Hoffmann, T., Valverde, J., Gonzalez, D., Riekkola, M. L., Kulmala, M., and Lelieveld, J.: The summertime Boreal forest field measurement intensive (HUMPPA-COPEC-2010): an overview of meteorological and chemical influences, Atmospheric Chemistry and Physics, 11, 10599-10618, 10.5194/acp-11-10599-2011, 2011.

Wong, K. W., Tsai, C., Lefer, B., Haman, C., Grossberg, N., Brune, W. H., Ren, X., Luke, W., and Stutz, J.: Daytime HONO vertical gradients during SHARP 2009 in Houston, TX, Atmospheric Chemistry and Physics, 12, 635-652, 10.5194/acp-12-635-2012, 2012.

Wong, K. W., Tsai, C., Lefer, B., Grossberg, N., and Stutz, J.: Modeling of daytime HONO vertical gradients during SHARP 2009, Atmos. Chem. Phys., 13, 3587-3601, 10.5194/acp-13-3587-2013, 2013.

Yabushita, A., Enami, S., Sakamoto, Y., Kawasaki, M., Hoffmann, M. R., and Colussi, A. J.: Anion-Catalyzed Dissolution of NO_2 on Aqueous Microdroplets, The Journal of Physical Chemistry A, 113, 4844-4848, 10.1021/jp900685f, 2009.

York, D., Evensen, N. M., Martínez, M. L., and De Basabe Delgado, J.: Unified equations for the slope, intercept, and standard errors of the best straight line, American Journal of Physics, 72, 367-375, doi:http://dx.doi.org/10.1119/1.1632486, 2004.

Zhang, N., Zhou, X., Bertman, S., Tang, D., Alaghmand, M., Shepson, P. B., and Carroll, M. A.: Measurements of ambient HONO concentrations and vertical HONO flux above a northern Michigan forest canopy, Atmospheric Chemistry and Physics, 12, 8285-8296, 10.5194/acp-12-8285-2012, 2012.

Zhou, X. L., Gao, H. L., He, Y., Huang, G., Bertman, S. B., Civerolo, K., and Schwab, J.: Nitric acid photolysis on surfaces in low-NO_x environments: Significant atmospheric implications, Geophysical Research Letters, 30, 2217   10.1029/2003gl018620, 2003.

Zhou, X. L., Zhang, N., TerAvest, M., Tang, D., Hou, J., Bertman, S., Alaghmand, M., Shepson, P. B., Carroll, M. A., Griffith, S., Dusanter, S., and Stevens, P. S.: Nitric acid photolysis on forest canopy surface as a source for tropospheric nitrous acid, Nat. Geosci., 4, 440-443, 10.1038/ngeo1164, 2011.

Zhu, C., Xiang, B., Zhu, L., and Cole, R.: Determination of absorption cross sections of surface-adsorbed HNO_3 in the 290–330 nm region by Brewster angle cavity ring-down spectroscopy, Chem. Phys. Lett., 458, 373-377, http://dx.doi.org/10.1016/j.cplett.2008.04.125, 2008.

Zhu, C. Z., Xiang, B., Chu, L. T., and Zhu, L.: 308 nm Photolysis of Nitric Acid in the Gas Phase, on Aluminum Surfaces, and on Ice Films, Journal of Physical Chemistry A, 114, 2561-2568, 10.1021/jp909867a, 2010.
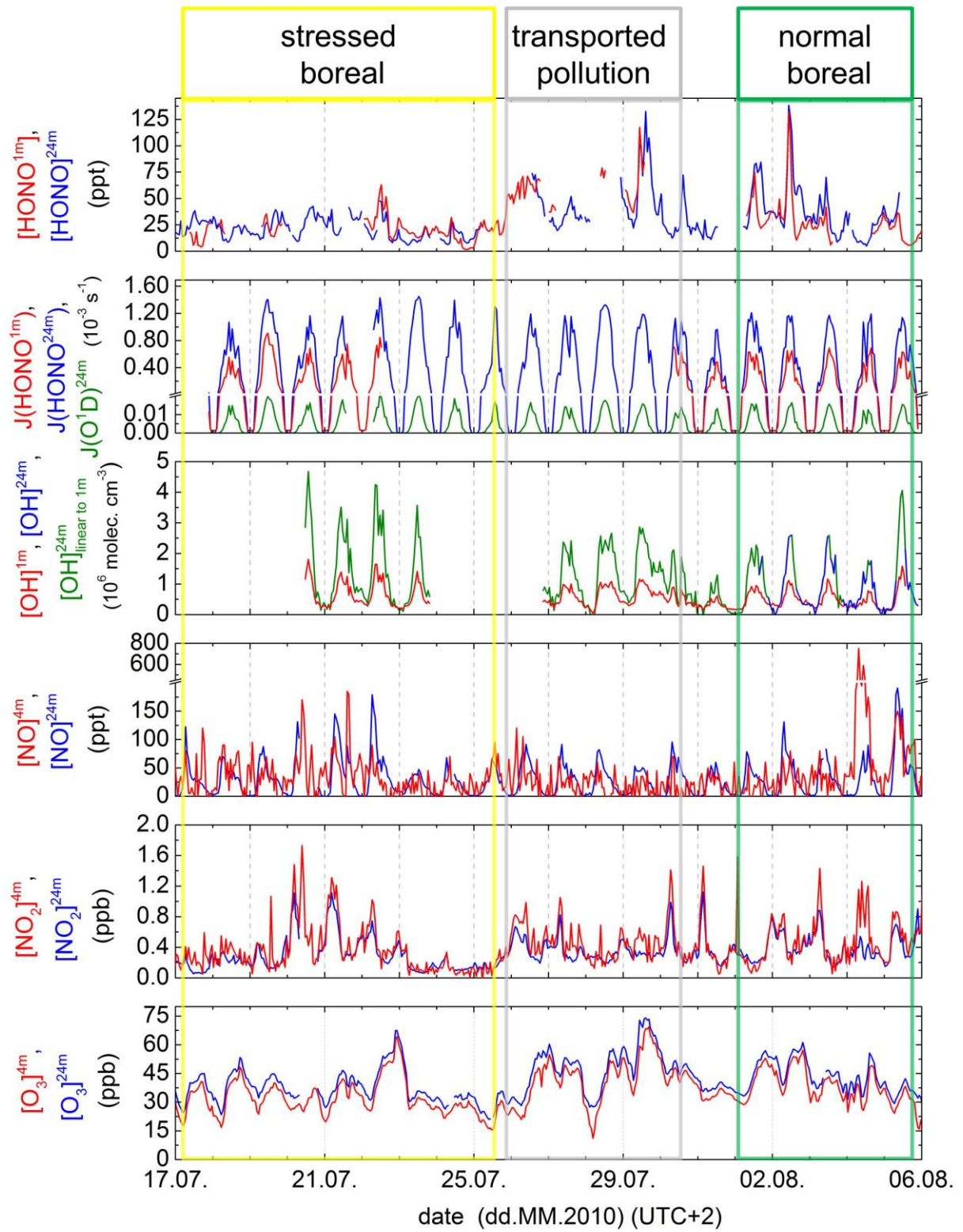
1
2 Figure 1. Overview of the measured concentration of different trace gases and the photolysis
3 frequencies J(HONO) and J(O¹D). The linearly connected data points represent 60 min
4 average values. Mixing ratios or concentrations are shown for the period where HONO was
5 measured at both heights. $[OH]^{24m}_{linear\ to\ 1m}$ was used to fill the gaps in OH measurements above

1   the canopy (see Fig. 2 a). Coloured boxes mark the respective regimes of "normal boreal"

2   (green), "stressed boreal" (yellow) and "transported pollution" (grey).

3
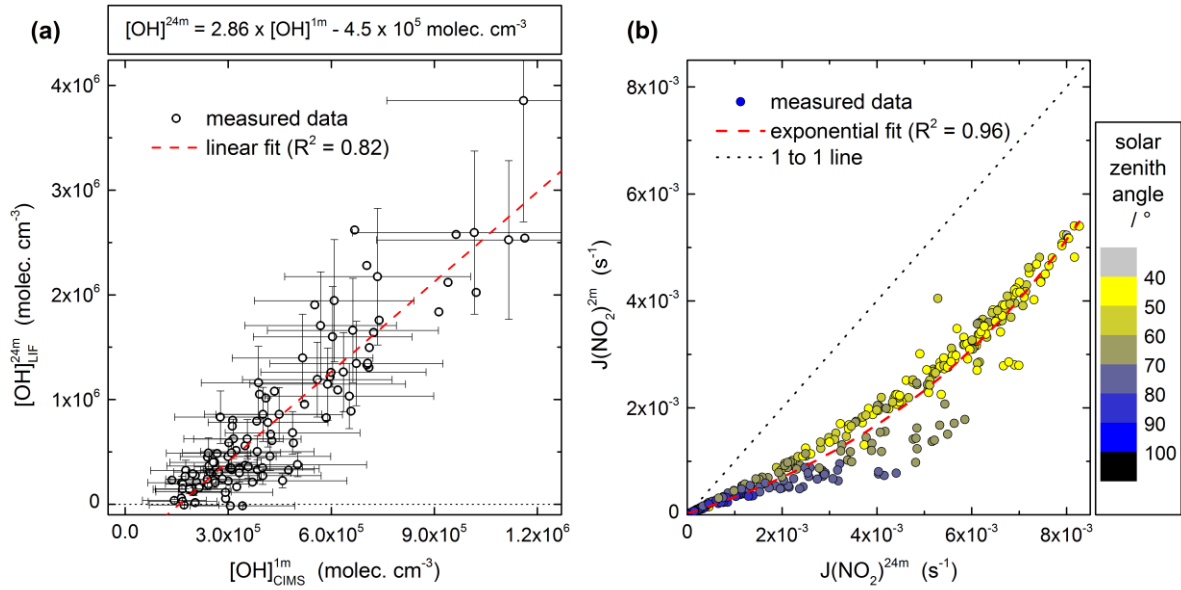
4
5   Figure 2. (A) The linear correlation of OH concentration below and above the canopy was

6   used for interpolating data of OH concentration above the canopy. (B) Similar to (A) the

7   exponential correlation of measured photolysis frequency below and above the canopy was

8   used to interpolate data of $J(NO_2)$ below the canopy. Color code of dots represents the solar

9   zenith angle. Additionally the 1 to 1 line is shown as dashed line.

10
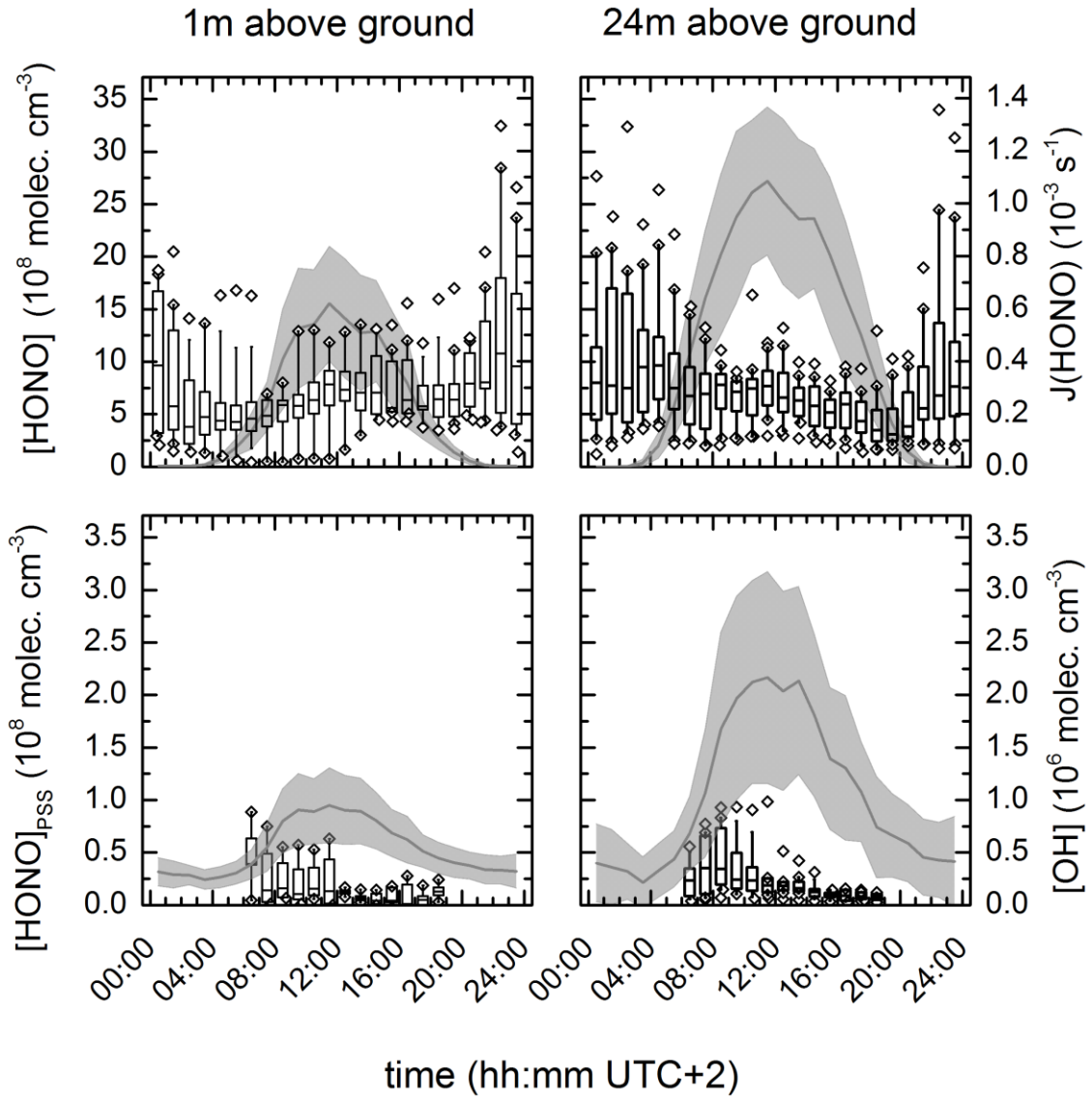
1
2 Figure 3. Upper panels show box plots of the diel cycle of HONO measured at 1 m and 24 m,
3 respectively and the average corresponding J(HONO) with standard deviation (grey shaded
4 line). Lower panels show box plots for the calculated PSS concentration of HONO for the
5 heights of 1 m and 24 m, respectively, during daytime (lifetime of HONO below 4 h) where
6 PSS is possibly attained. Additionally, the average concentration of OH with standard
7 deviation (grey shaded line) for the two respective heights is presented. The boxes represent
8 the 25 to 75 percentile, the line within the box is the median, the bars show the 10 to 90
9 percentile and outliers are marked as open diamonds.

10

1
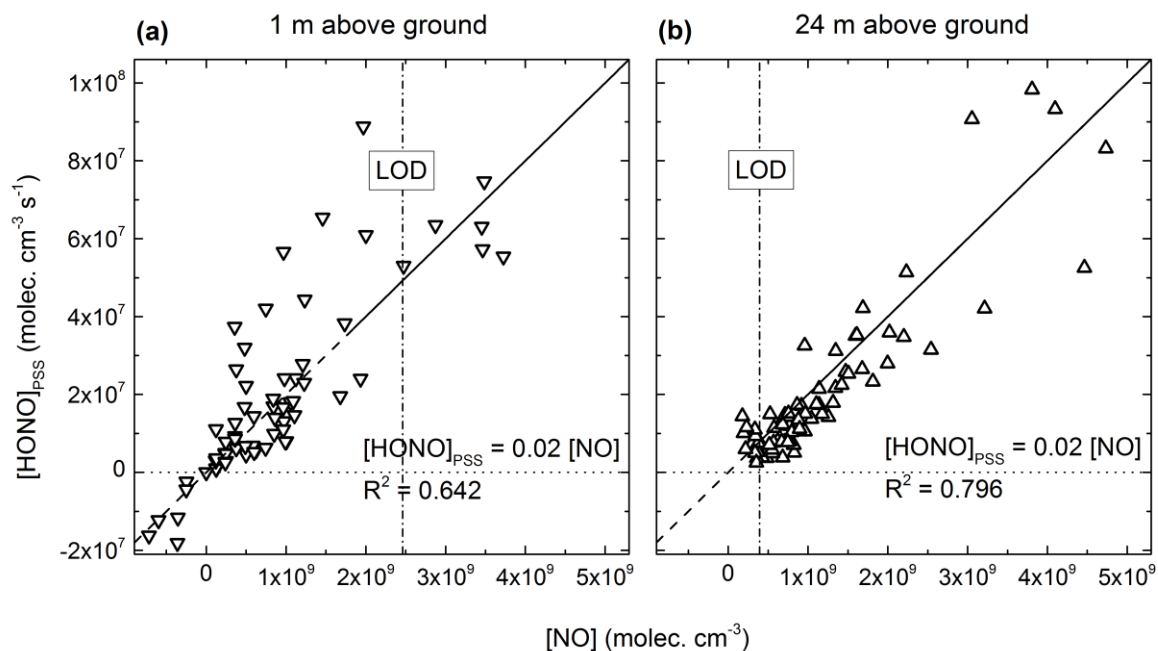
2 Figure 4. The PSS concentration of HONO, $[HONO]_{PSS}$, at 1 m measurement height (a) and

3 at 24 m measurement height (b) is plotted against the concentration of NO at the

4 corresponding heights. The dashed-dotted vertical line reflects the lower limit of detection

5 (LOD) for each NO measurement. The linear fit using a fixed slope of 0.02 and no offset

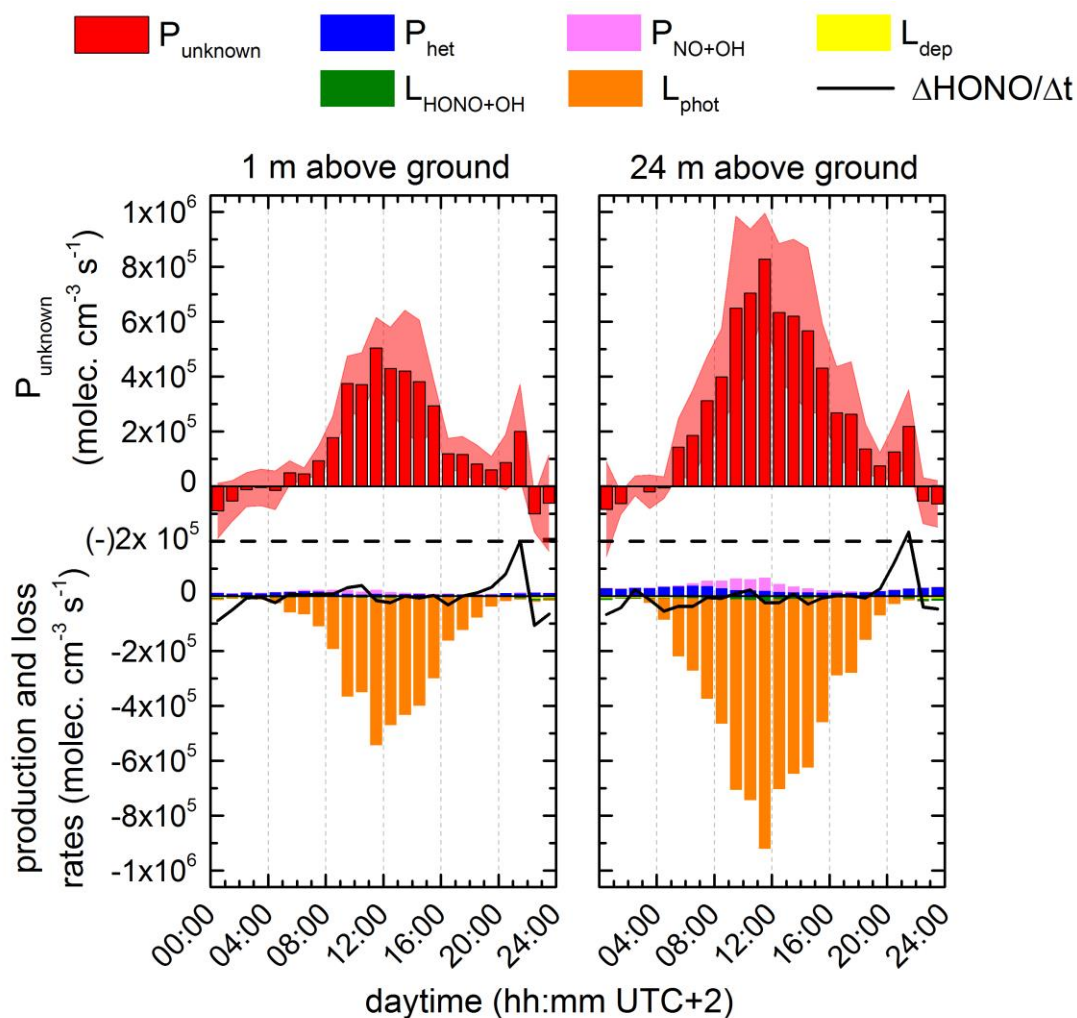6 leads to a reasonable correlations between $[HONO]_{PSS}$ and [NO] in both cases.

7

1
2 Figure 5. The diel variation of $P_{unknown}$ (red bars, upper panel) with standard deviation (red
3 shade), the single production and loss terms (coloured bars, lower panel) and the change in
4 HONO concentration ($\Delta HONO/\Delta t$) (black line, lower panel) for the two heights are shown.
5 The scales and units at the left and right hand y-axis are valid for both measurement heights
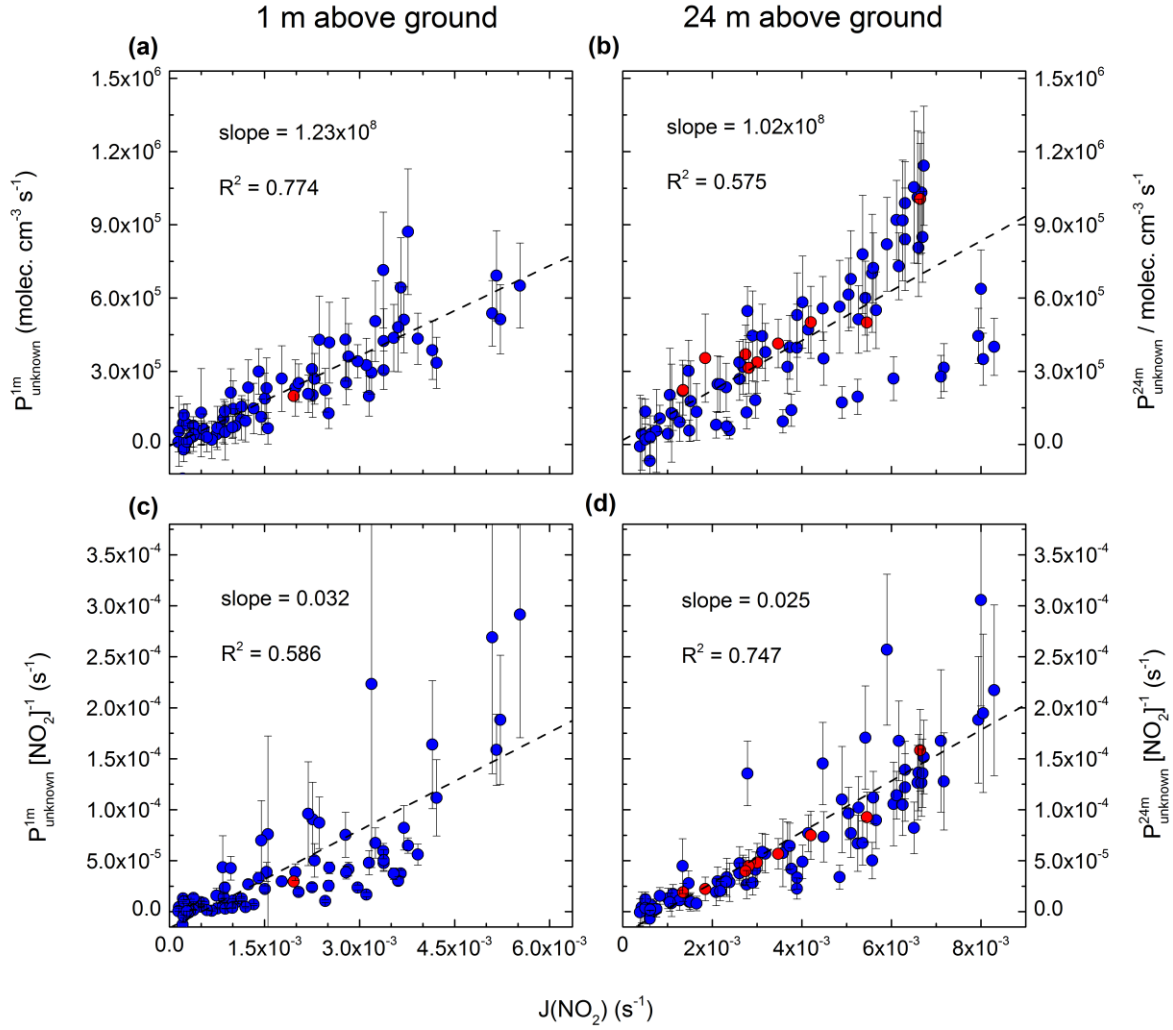6 and were chosen for an easy comparison with other publications.

7

Figure 6. In the upper panels, (a) and (b), $P_{unknown}$ for both measurement heights is linearly correlated with corresponding $J(NO_2)$. In the lower panels, (c) and (d), $P_{unknown}$ is scaled by the NO_2 concentration and still linearly correlated with $J(NO_2)$. Blue dots denote budget data availability at both heights, whereas red dots are available only at the respective measurement height. Linear fits refer to total data available (blue and red),
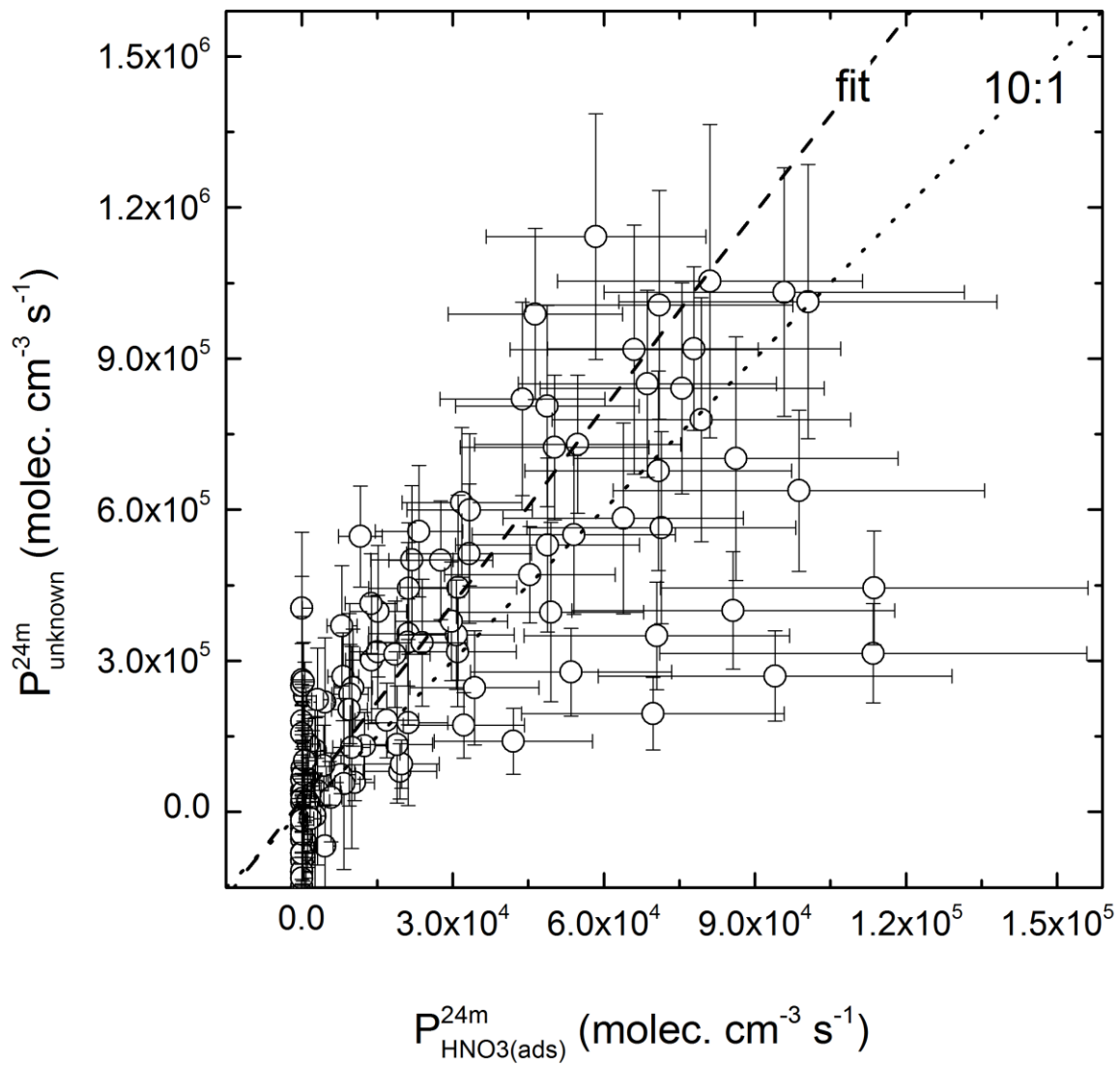
1
2 Figure 7. $P_{unknown}$ at the measurement height of 24 m during daytime is plotted against the
3 production of HONO from photolysis of adsorbed HNO_3 on leaf surfaces, $P_{HNO3(ads)}$. With an
4 enhancement factor of 43 and a surface loading of $(8.3 \pm 3.1) \times 10^{-5}$ mol m^{-2} it might explain
5 up to 10 % of $P_{unknown}$, indicated by the 10 to 1 line (dotted line). The York linear fit (York et
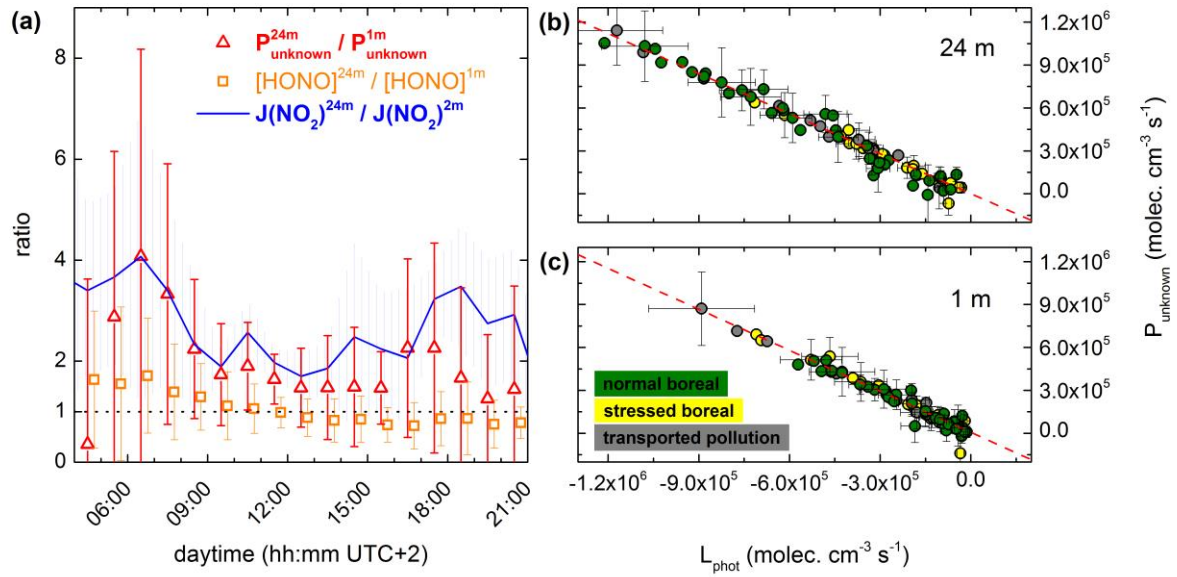6 al., 2004) yields in $P_{unknown} = (12.9 \pm 1.0) \times P_{HNO3(ads)} + (2.4 \pm 1.1) \times 10^4$ molecules cm^{-3} s^{-1}.

7

1

2 Figure 8. (a) The average ratio of $P_{unknown}^{24m}$ to $P_{unknown}^{1m}$ (red triangles), the average ratio of

3 $[HONO]^{24m}$ to $[HONO]^{1m}$ (orange squares) and the average ratio of $J(NO_2)^{24m}$ to $J(NO_2)^{2m}$

4 (blue line) change during daytime (lifetime of HONO < 4 h). For clarity a second x-

5 coordinate for the ratio of $[HONO]^{24m}$ to $[HONO]^{1m}$ is used with a shift of +15 min, but is not

6 shown. (b) $P_{unknown}^{24m}$ and (c) $P_{unknown}^{1m}$ are plotted against the photolytic loss rate of HONO at

7 24 m and 1 m above ground, respectively, colour codes mark the respective regimes of

8 "normal boreal" (green), "stressed boreal" (yellow) and "transported pollution" (grey). The

9 York linear fit (York et al., 2004) of $P_{unknown}^{24m}$ with L_{phot}^{24m} and $P_{unknown}^{1m}$ with L_{phot}^{1m} yields in

10 $P_{unknown}^{24m} = - (0.93 \pm 0.05)$ x $L_{phot}^{24m} + (0.9 \pm 14.2)$ x 10^3 molecules cm^{-3} s^{-1} and $P_{unknown}^{1m} = -$

11 (0.96 ± 0.08) x $L_{phot}^{1m} + (0.6 \pm 11.9)$ x 10^3 molecules cm^{-3} s^{-1}, respectively.

12